© 2014. Published by The Company of Biologists Ltd | Journal of Cell Science (2014) 127, 2910–2919 doi:10.1242/jcs.147785

RESEARCH ARTICLE

Ccdc13 is a novel human centriolar satellite protein required for ciliogenesis and genome stability

Christopher J. Staples[1], Katie N. Myers[1], Ryan D. D. Beveridge[1], Abhijit A. Patil[1], Anna E. Howard[1], Giancarlo Barone[1], Alvin J. X. Lee[2], Charles Swanton[2], Michael Howell[3], Sarah Maslen[4], J. Mark Skehel[4], Simon J. Boulton[5] and Spencer J. Collis[1,*]

ABSTRACT

Here, we identify coiled-coil domain-containing protein 13 (Ccdc13) in a genome-wide RNA interference screen for regulators of genome stability. We establish that Ccdc13 is a newly identified centriolar satellite protein that interacts with PCM1, Cep290 and pericentrin and prevents the accumulation of DNA damage during mitotic transit. Depletion of Ccdc13 results in the loss of microtubule organisation in a manner similar to PCM1 and Cep290 depletion, although Ccdc13 is not required for satellite integrity. We show that microtubule regrowth is enhanced in Ccdc13-depleted cells, but slowed in cells that overexpress Ccdc13. Furthermore, in serum-starved cells, Ccdc13 localises to the basal body, is required for primary cilia formation and promotes the localisation of the ciliopathy protein BBS4 to both centriolar satellites and cilia. These data highlight the emerging link between DNA damage response factors, centriolar and peri-centriolar satellites and cilia-associated proteins and implicate Ccdc13 as a centriolar satellite protein that functions to promote both genome stability and cilia formation.

KEY WORDS: Ccdc13, Centriolar satellites, Ciliogenesis, Genome stability

INTRODUCTION

The mammalian centrosome is a major site of microtubule nucleation and organisation during both interphase and mitosis, and is also the origin of primary cilia formation. Furthermore, it is important for establishing a mitotic spindle in order to ensure efficient chromosome segregation and genome stability. The mammalian centrosome comprises two orthogonally orientated microtubule barrels called centrioles, which are surrounded by a mesh of electron-dense pericentriolar material (PCM). This, in part, comprises particles termed centriolar satellites. The formation of an organised microtubule array is dependent on satellite proteins, such as pericentriolar material 1 (PCM1), which is thought to act as a scaffold to recruit other proteins – including pericentrin, ninein, Cep90 and Cep290 to the PCM (Dammermann and Merdes, 2002; Kim and Rhee, 2011; Lopes et al., 2011; Mogensen et al., 2000). This involves complex and incompletely characterised interactions between numerous satellite proteins and the dynein–dynactin microtubule minus-end motor system (Dammermann and Merdes, 2002; Kim et al., 2008; Kim et al., 2004; Kodani et al., 2010; Lee and Rhee, 2010).

A number of centriolar satellite proteins, such as PCM1 and the ciliopathy proteins Cep290 and Bardet-Biedl syndrome protein 4 (BBS4) cooperate in the formation of the primary cilia (Kim et al., 2008; Lopes et al., 2011; Stowe et al., 2012), an organelle that has only recently been appreciated as a crucial signalling hub for a number of pathways, which include Wnt and sonic hedgehog (Logan et al., 2011). Recent work has demonstrated that a number of proteins involved in the DNA damage response (DDR) also function during ciliogenesis. Mutations in Mre11, ZNF423 and Cep164 are causative of a subset of renal ciliopathies (Chaki et al., 2012), whereas FAN1 mutations cause karyomegalic interstitial nephritis (Zhou et al., 2012). Interestingly, the DDR kinase ATR has been shown recently to localise to the photoreceptor connecting cilium, and ATR-deficient mice exhibit ciliary defects and photoreceptor degeneration (Valdés-Sánchez et al., 2013). Furthermore, it has been demonstrated recently that the renal-ciliopathy-associated kinase Nek8 also plays a role in ATR signalling during the cellular responses to replication stress (Choi et al., 2013). Finally, mutations in several DNA replication factors impair ciliogenesis and are causative of Meier-Gorlin syndrome (Stiff et al., 2013).

In a recent human genome-wide small interfering (si)RNA-based screen investigating regulators of genome stability, we identified Cep131, a protein that is required for both cilia formation and genome integrity (Staples et al., 2012). Through our ongoing analyses of candidates identified in this screen, the uncharacterised protein coiled-coil domain-containing protein 13 (Ccdc13) has been identified as a potential regulator of genome stability. We report here that Ccdc13 is a novel centriolar satellite protein that is required for cilia formation and genome stability. Depletion of Ccdc13 results in increased levels of post-mitotic DNA damage. At the molecular level, Ccdc13 binds to a number of satellite proteins – including PCM1, Cep290, pericentrin and Cep131 – and its depletion causes defects in ciliogenesis and the reduced recruitment of BBS4 to centriolar satellites. The modulation of Ccdc13 levels also alters microtubule organisation in interphase cells and microtubule regrowth following depolymerisation. Consistent with recent findings – that mutations in several DDR proteins give rise to human ciliopathies – our data reveal that an emerging subset of centriolar

[1]Genome Stability Group, CR-UK/YCR Sheffield Cancer Research Centre, Department of Oncology, Academic Unit of Molecular Oncology, University of Sheffield Medical School, Beech Hill Road, Sheffield S10 2RX, UK. [2]Translational Cancer Therapeutics Laboratory, Cancer Research UK London Research Institute, 44 Lincoln's Inn Fields, London WC2A 3LY, UK. [3]High Throughput Screening Facility, CR-UK London Research Institute, 44 Lincoln's Inn Fields London, WC2A 3LY, UK. [4]Mass Spectrometry Group, The MRC Laboratory of Molecular Biology, Division of Cell Biology, Hills Road, Cambridge, CB2 0QH, UK. [5]DNA CR-UK Damage Response Laboratory, London Research Institute, Clare Hall Laboratories, South Mimms, EN6 3LD, UK.

*Author for correspondence (s.collis@sheffield.ac.uk)

Received 9 December 2013; Accepted 28 April 2014

Journal of Cell Science

Journal of Cell Science (2014) 127, 2910–2919 doi:10.1242/jcs.147785

satellite proteins function both to promote ciliogenesis and to maintain genome stability.

RESULTS

Identification and validation of Ccdc13 as a novel regulator of genome stability

We have recently carried out a genome-wide siRNA screen to identify novel regulators of genome stability (Staples et al., 2012) by using phosphorylation of the histone variant H2AX on Ser139 (termed γH2AX) as a marker of increased DNA damage (Bonner et al., 2008). As part of this screen, we identified Ccdc13, which yielded a high Z-score of 2.2. Ccdc13 is a structural maintenance of chromosomes (SMC)-domain-containing protein, which is encoded on the short arm of chromosome 3 in humans (3p22.1) and is conserved in primate, dog, cow, rat, chicken and zebrafish.

To confirm the screen data (which was performed in the human colorectal cell line HCT116 using a small interfering (si)RNA pool comprising four different oligonucleotides), we transfected HeLa cells (derived from a cervical carcinoma) with four individual siRNAs that targeted Ccdc13. All four siRNAs resulted in an increased number of cells that exhibited γH2AX foci (Fig. 1A), thus validating the outcome of the initial screen and strongly diminishing the likelihood that the results were the consequence of off-target effects of the siRNA. In order to confirm efficient knockdown of Ccdc13, we tested two different commercially available antibodies against Ccdc13 in combination with siRNA transfections. However, neither antibody recognised endogenous Ccdc13, and both only weakly recognised overexpressed Ccdc13 (data not shown). Therefore, we confirmed that all four Ccdc13-directed siRNA conferred efficient knockdown of exogenous forms of Ccdc13 (supplementary material Fig. S1A). Additionally, we confirmed that two Ccdc13 siRNA, which we use for all subsequent studies, resulted in a significant reduction of endogenous *Ccdc13* mRNA levels, as assessed by using quantitative RT-PCR (supplementary material Fig. S1B).

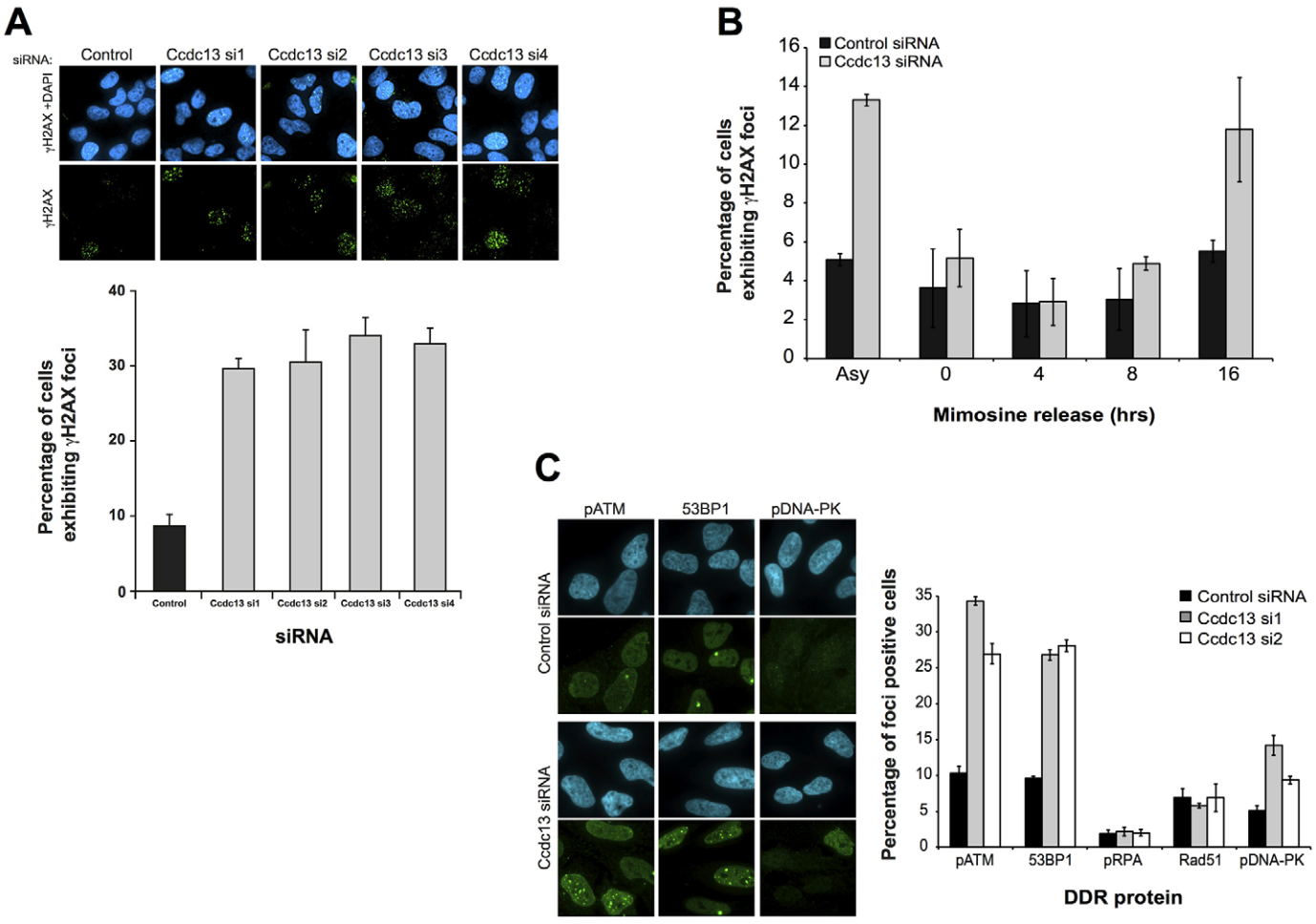

Fig. 1. Depletion of Ccdc13 results in increased post-mitotic DNA damage. (A) HeLa cells were transfected with non-targeting control siRNA, or four individual siRNAs (si1–si4) that targeted Ccdc13, as indicated. After 48 h, the cells were fixed, stained for γH2AX and counterstained with DAPI (blue, upper panel), and cells containing >5 foci were quantified from three independent experiments (lower panel). (B) HCT116 cells were transfected with non-targeting control or Ccdc13-targeting siRNA. After 48 h, the cells were treated with 300 μM mimosine for 24 h then released into normal medium for the indicated times. Cells were then fixed, stained for γH2AX and counterstained with DAPI. The data shown represents the quantification of cells that contained >5 γH2AX foci in three independent experiments. (C) HeLa cells were transfected with non-targeting control siRNA, or two individual siRNA targeted Ccdc13. After 48 h, these cells were stained for either phosphorylated RPA (at residue Thr21; pRPA), phosphorylated ATM (at residue Ser1981; pATM), phosphorylated DNA-PK (at residue Thr2609; pDNA-PK), Rad51 or 53BP1 and counterstained with DAPI. Cells with >5 foci indicating sites of damage or replication stress were counted and displayed as a percentage of the total number of cells. All experiments were performed at least three times, error bars represent the standard error of the means and representative images are shown of pATM, 53BP1 and pDNA-PK staining.

Journal of Cell Science (2014) 127, 2910–2919 doi:10.1242/jcs.147785

Increased amounts of endogenous DNA damage can arise as a consequence of defective DDR signalling (Chapman et al., 2012). Therefore, we assessed the phosphorylation of the DDR effector kinases Chk1 and Chk2 (also known as CHEK1 and CHEK2, respectively) following exposure to hydroxyurea and ionising radiation, we then assessed the effect of Ccdc13 depletion on cell survival following these treatments. Neither effector kinase phosphorylation, nor cell survival, was altered by depletion of Ccdc13 (supplementary material Fig. S1C; data not shown), suggesting that Ccdc13 does not play a substantial role in the activation and/or maintenance of the DDR. To ascertain the origin of the increased DNA damage that we observed in Ccdc13-depleted cells, we performed cell-cycle block–release experiments using the iron chelator mimosine, which induces cell-cycle arrest in G1 phase without leading to centrosome over-duplication (Prosser et al., 2009). The treatment of cells with mimosine supressed the increased formation of γH2AX foci that we observed following Ccdc13 depletion (Fig. 1B). Furthermore, in a similar manner to that previously reported for Cep131 (Staples et al., 2012), increased γH2AX was only observed in Ccdc13-depleted cells in G1 following mitotic transit (Fig. 1B). However, in contrast with our findings with Cep131, the depletion of Ccdc13 did not cause centrosome amplification or alterations in the size of the pericentriolar material (PCM; data not shown).

To investigate how Ccdc13-depleted cells respond to the increased endogenous DNA damage, we assessed the formation of nuclear foci comprising phosphorylated ATM, 53BP1 (also known as TP53BP1), Rad51, phosphorylated RPA and phosphorylated DNA-dependent protein kinase (DNA-PK) (Bekker-Jensen et al., 2006). Consistent with the increased amounts of DNA damage in Ccdc13-depleted cells (Fig. 1A), the depletion of Ccdc13 led to a considerable increase in the number of cells that exhibited activated ATM (indicated by phosphorylation at Ser1981), activated DNA-PK (phosphorylated at Thr2609) and 53BP1 nuclear foci compared with cells that had been treated with control siRNA (Fig. 1C). However, the percentage of cells that showed foci of Rad51 or activated RPA (phosphorylated at Thr21) was unaltered in Ccdc13-depleted cells compared with those that had been transfected with control siRNA (Fig. 1C). These data suggest that cells deficient in Ccdc13 generate DNA breaks during mitosis, and given the non-toxic effects of Ccdc13 depletion, we predict that the majority of these lesions are repaired by non-homologous end joining (NHEJ) in the subsequent G1 phase of the cell cycle (Chapman et al., 2012; Giunta et al., 2010). Indeed, an increased percentage of Ccdc13-depleted cells exhibited micronuclei (supplementary material Fig. S1D), which are a marker of post-mitotic DNA damage (Janssen et al., 2011). The post-mitotic repair of such lesions would also be consistent with the notion that the DDR is preserved in Ccdc13-depleted cells (supplementary material Fig. S1C). It is worth noting that these phenotypes are a result of substantially reduced levels of Ccdc13 and might be more severe following complete loss (knockout) of the endogenous protein.

Ccdc13 is a novel human centriolar satellite protein

To gain insight into the molecular function of Ccdc13, we generated both HeLa and HEK293 cell lines that stably expressed tetracycline-inducible Ccdc13 that was tagged at the N-terminus with FLAG or yellow fluorescent protein (YFP) (supplementary material Fig. S2A). In interphase cells that expressed low levels of YFP–Ccdc13, Ccdc13 localised to the centriolar core region – as evidenced by strong colocalisation with γ-tubulin (Fig. 2A). However, in cells that expressed high amounts of YFP–Ccdc13, it also localised diffusely around the centrosome in an array reminiscent of centriolar satellites. Indeed, the YFP–Ccdc13 structures colocalised strongly with the archetypal centriolar satellite PCM1 (Fig. 2A). Furthermore, immunofluorescent analysis of cells that expressed ectopic Ccdc13 that had a Myc tag at the N-terminus (supplementary material Fig. S2A) also demonstrated substantial colocalisation of tagged Ccdc13 and PCM1 (Fig. 2A). In keeping with the range of known centrosomal proteins that, like Ccdc13, contain at least one SMC domain, further examination of YFP–Ccdc13-expressing cells, by using immunofluorescence, confirmed that Ccdc13 is a centrosomal protein with dynamic localisation. As cells traversed interphase, YFP–Ccdc13 expression became more restricted in localisation to both of the separating centrosomes through the late-G2 phase (Fig. 2B). In early mitosis, YFP–Ccdc13 localised to both spindle poles and remained there during metaphase and anaphase (Fig. 2B), although there was a qualitative suggestion that this localisation might be somewhat diminished following metaphase. However, owing to a lack of antibodies that strongly recognise Ccdc13, it is unclear whether this is representative of endogenous Ccdc13, or whether the persistence of YFP–Ccdc13 at anaphase spindle poles is an artefact of overexpression. As cells progress through telophase and cytokinesis, YFP–Ccdc13 once again assumed a centriolar satellite distribution in both daughter cells (Fig. 2B).

Centrosomal localisation of satellites is often dependent on the presence of intact microtubules and a functional dynein–dynactin transport system (Dammermann and Merdes, 2002; Staples et al., 2012). To determine if a similar mechanism might underlie Ccdc13 recruitment to centrosomes, we disrupted microtubules using the microtubule depolymerising agent nocodazole. The treatment of cells with nocodazole caused a marked disruption to the centrosomal localisation of Ccdc13 (Fig. 2C). Consistent with this finding, the disruption of microtubules by using treatments with ice also led to the dispersal of Ccdc13 from the centrosome (data not shown). PCM1 is transported to the centrosome through the dynein–dynactin transport system, through which it also carries protein cargos to the centrosome (Dammermann and Merdes, 2002). Therefore, we assessed the effect of disruption of the dynactin transport system on the centrosomal localisation of Ccdc13. Overexpression of p50-dynamitin (also known as DCTN2), which disrupts the dynactin transport system, caused mislocalisation of YFP–Ccdc13 from the centrosome (Fig. 2C), suggesting that Ccdc13 is itself a protein cargo for PCM1-mediated transport.

The dynamic cell-cycle localisation of Ccdc13 coupled with mislocalisation following microtubule disruption provides further evidence that Ccdc13 is a centriolar satellite protein. Indeed, tetracycline-inducible YFP–Ccdc13 almost exclusively colocalised with the centriolar satellite protein Cep215 and the centriolar sub-distal appendage protein Cep170 in both interphase (G1) cells and in late-G2–early mitotic cells (supplementary material Fig. S2B). Furthermore, we found that depletion of PCM1 caused complete disruption of the centriolar satellite localisation of Ccdc13 (Fig. 2D); an observation that is consistent with the known role of PCM1 in satellite formation through the loading of dynein protein cargoes (Dammermann and Merdes, 2002; Lopes et al., 2011). Interestingly, we found that PCM1 depletion did not affect the localisation of a subset of Ccdc13, which

Journal of Cell Science (2014) 127, 2910–2919 doi:10.1242/jcs.147785

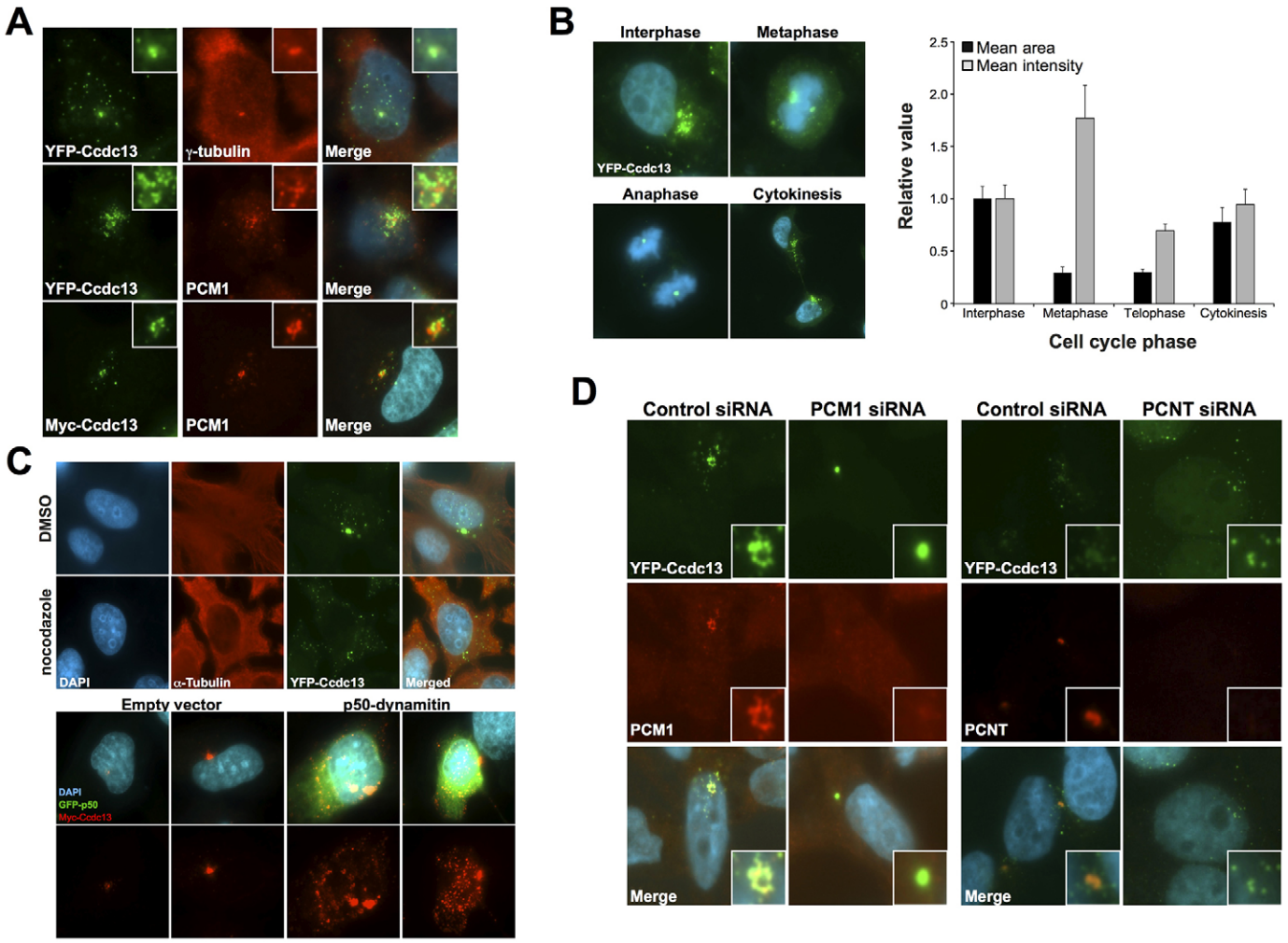

Fig. 2. Fluorescently tagged Ccdc13 localises to centriolar satellites in a PCM1- and pericentrin-dependent manner. (A) Top two rows: HeLa cells that stably expressed tetracycline-inducible YFP-tagged Ccdc13 (supplementary material Fig. S2A) were treated with 1 μg/ml tetracycline to induce Ccdc13 expression, for 24 h. Bottom row: additionally, HeLa cells were transfected with a plasmid expressing Myc–Ccdc13 (supplementary material Fig. S2A). Cells were fixed and co-stained for Myc or GFP and either γ-tubulin or PCM1, as indicated, then counterstained with DAPI (blue). The average Pearson's coefficient for colocalisation with PCM1 was calculated as 0.760 and 0.815 for YFP–Ccdc13 and Myc–Ccdc13, respectively. Inset images highlight the centrosome-satellite region for a given image. (B) Left panel: representative images of HeLa cells that stably expressed low amounts of tetracycline-inducible YFP-tagged Ccdc13 (fixed and stained for GFP) at various stages of the cell cycle. Right panel: quantification of the mean area occupied by, and the mean fluorescence intensity for, YFP–Ccdc13 (relative arbitrary units to interphase cells) at the various stages of the cell cycle. The error bars represent the standard deviation of the means. (C) Upper panel: YFP–Ccdc13-expressing HeLa cells were treated with 1 μg/ml nocodazole and fixed after 3 h, before staining for GFP and α tubulin and counterstaining with DAPI. Lower panels: cells were transfected with either empty vector and Myc–Ccdc13, or Myc–Ccdc13 and a vector encoding GFP-tagged p50-dynamitin. After 24 h, cells were fixed and stained with antibodies against GFP and Myc and then counterstained with DAPI. (D) YFP–Ccdc13 cells were transfected with non-targeting control siRNA, or siRNA that targeted PCM1 or pericentrin (PCNT), as indicated. After 48 h, 1 μg/ml tetracycline was added to induce YFP–Ccdc13 expression and after a further 24 h cells were fixed, stained for GFP and PCM1 or PCNT and counterstained with DAPI. All experiments were performed three times, and representative images are shown throughout. Inset images highlight the centrosome-satellite region for a given image.

remained at the centriolar core; a finding similar to that observed for the centriolar satellite protein Cep131 (Staples et al., 2012). In a manner similar to Cep131, depletion of pericentrin (also known as PCNT) resulted in the complete disruption of Ccdc13 localisation from both the centriolar core and the pericentriolar satellites (Fig. 2D).

Centrosomal satellites often form multimeric protein complexes (Bärenz et al., 2011). Therefore, to further define Ccdc13 as a newly identified centrosomal satellite protein, we carried out proteomic analyses of FLAG–Ccdc13 complexes that had been purified from tetracycline-inducible HEK293 stable cell lines (supplementary material Fig. S2A). Proteins that, putatively, interacted with Ccdc13 with the greatest peptide coverage were PCM1, pericentrin, Cep290, Cep215, Cep131, Cep90 and Cep72 (Fig. 3A), which have all been previously shown to localise to centriolar satellites (Balczon et al., 1994; Dammermann and Merdes, 2002; Kim et al., 2008; Kim et al., 2012; Lee and Rhee, 2010; Lopes et al., 2011; Ma and Jarman, 2011; Stowe et al., 2012). Additionally, we confirmed that YFP–Ccdc13 colocalised with PCM1 and pericentrin (Fig. 3B), and that FLAG–Ccdc13 interacts with endogenous pericentrin, PCM1 and Cep290 (Fig. 3C). Furthermore, reciprocal experiments in which the satellite proteins PCM1, pericentrin, Cep290 and Cep131 were immunoprecipitated from HeLa cells that stably expressed

Journal of Cell Science (2014) 127, 2910–2919 doi:10.1242/jcs.147785

A

Gene symbol	No. Unique peptides - Tet	+ Tet	Peptide coverage
PCM1	0	35	18 %
Cep131	0	18	16 %
Cep90	0	16	23 %
Cep350	0	13	4.9 %
Ccdc13	2	20	32 %
Cep170	1	10	8.4 %
PCNT	0	9	2.9 %
Cep215	1	7	4.9%
Cep135	1	5	4.5 %
Cep72	0	3	5.9 %
Cep290	0	3	1.4 %
Ccdc77	0	3	8.3 %
Ccdc61	0	3	5.5 %
Ccdc18	0	3	1.5 %
Ccdc14	0	2	2.8 %
APC1	0	2	1.3 %

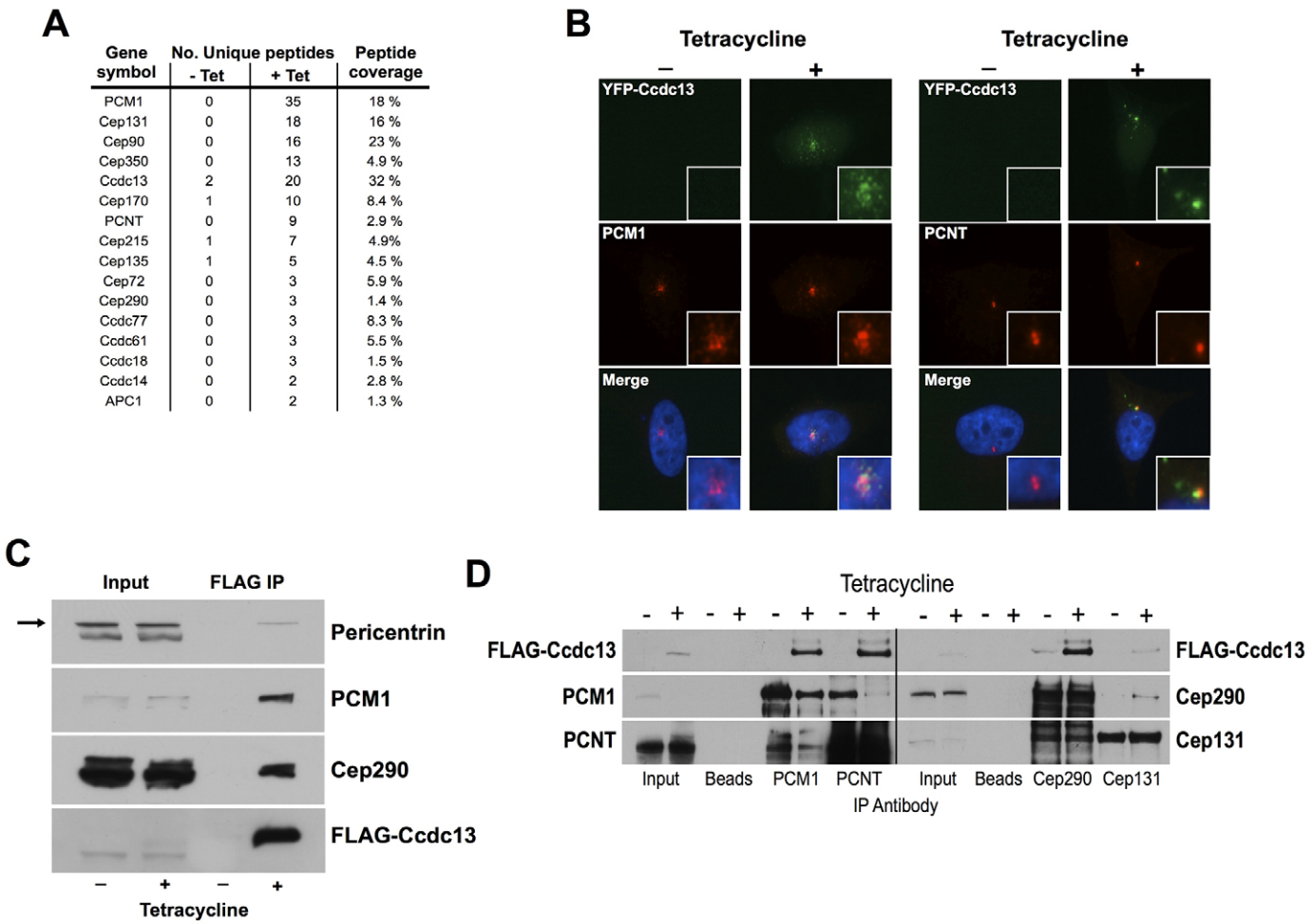

Fig. 3. Ccdc13 interacts and colocalises with several centriolar satellite proteins. (A) HEK293 cells that stably expressed tetracycline-inducible FLAG-tagged Ccdc13 (supplementary material Fig. S2A) were grown in large-scale culture. Cells were mock-treated, or 1 μg/ml tetracycline was added to induce FLAG–Ccdc13 expression, and after 24 h, the cells were lysed and FLAG–Ccdc13 was immunoprecipitated using FLAG M2 antibody conjugated to agarose beads. FLAG–Ccdc13 was eluted using 150 ng/ml 3×FLAG peptide, and the resulting eluates were boiled and resolved by SDS-PAGE. Following SYPRORuby staining, the gel was dissected, and the proteins were sent for mass spectrometry analysis. A shortlist of proteins that were significantly enriched in the tetracycline-induced sample (as evidenced by the enrichment of recovered unique peptides) is shown, alongside the associated peptide coverage. (B) YFP–Ccdc13-expressing HeLa cells were mock-treated, or treated with 1 μg/ml tetracycline to induce expression. After 24 h, the cells were fixed and stained for GFP and co-stained for either PCM1 or pericentrin (PCNT). Inset images highlight the centrosome-satellite region for a given image. (C) FLAG–Ccdc13-expressing HeLa cells were mock-treated or treated with 1 μg/ml tetracycline. After 24 h, the cells were lysed, and FLAG–Ccdc13 was immunoprecipitated (IP) using an antibody against FLAG that had been conjugated to agarose beads and then eluted with 3×FLAG peptide. Eluates were resolved by SDS-PAGE, and the blots were probed using antibodies against PCNT, PCM1, Cep290 and FLAG. (D) HeLa cells that stably expressed tetracycline-inducible FLAG-tagged Ccdc13 (supplementary material Fig. S2A) were mock-treated or treated with 1 μg/ml tetracycline. After 24 h, cells were lysed and immunoprecipitations were performed with Protein-G–Sepharose beads using antibodies against the centrosomal satellite proteins PCM1, PCNT, Cep290 and Cep131, as indicated. Eluates were resolved by SDS-PAGE, and western blotting was performed with the indicated antibodies. Beads, control reaction lacking antibody.

tetracycline-inducible FLAG-tagged Ccdc13 (supplementary material Fig. S2A) demonstrated strong interactions between these proteins and FLAG–Ccdc13 (Fig. 3D). Identical experiments that used a HeLa line expressing tetracycline-inducible YFP–Ccdc13 (supplementary material Fig. S2A) yielded the same results (supplementary material Fig. S2C). Collectively, these data are consistent with the notion of Ccdc13 being a *bone fide* centrosomal satellite protein.

Ccdc13 is required for microtubule organisation and ciliogenesis

PCM1 and Cep290 are required for the maintenance of a radial microtubule array in U2OS cells (Dammermann and Merdes, 2002; Kim et al., 2008). To assess whether Ccdc13 might have a similar role, we depleted U2OS cells of Ccdc13 and examined microtubule organisation by staining for α-tubulin. PCM1 siRNA was used as a positive control, and as expected, depletion of PCM1 resulted in a marked loss of microtubule organisation (Fig. 4A). Interestingly, Ccdc13 depletion caused a similar, but less marked, loss of interphase microtubule organisation (Fig. 4A), indicating that Ccdc13 plays a role in maintaining a stable microtubule array. Ccdc13-depleted cells also exhibited disrupted mitotic microtubules (supplementary material Fig. S3A); however, any such disruption to the mitotic spindle in Ccdc13-depleted cells did not appear to activate the spindle assembly checkpoint, as the duration of transit through mitosis was unaffected in Ccdc13-depleted cells, when assessed over multiple experiments (supplementary material Fig. S3B).

Journal of Cell Science (2014) 127, 2910–2919 doi:10.1242/jcs.147785

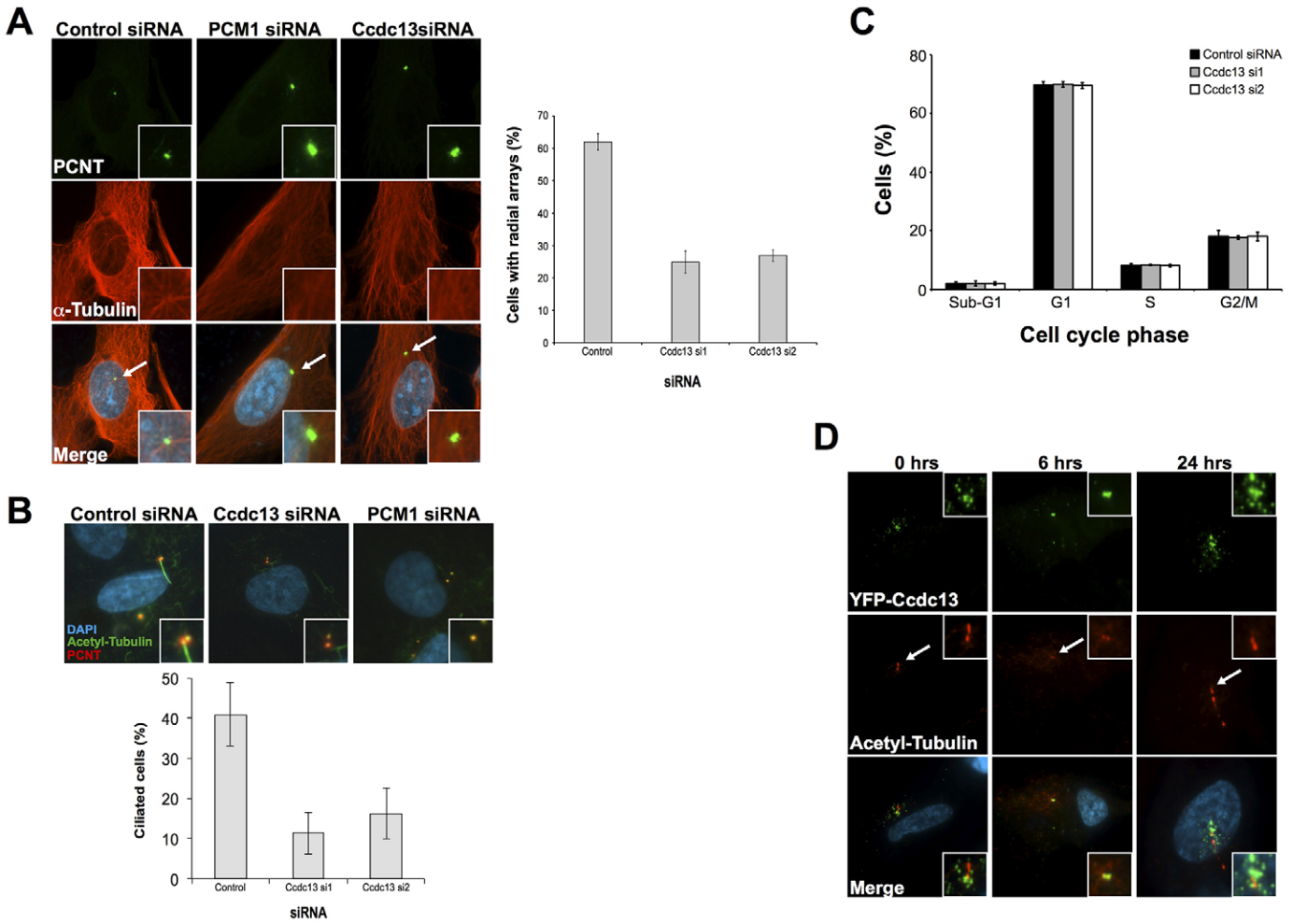

Fig. 4. Ccdc13 is required for interphasic microtubule organisation and ciliogenesis. (A) Microtubule organisation in U2OS cells that had been transfected with non-targeting control siRNA, or siRNA targeting Ccdc13. After 48 h, the cells were fixed, stained for pericentrin (PCNT) and α-tubulin and counterstained with DAPI (blue) to assess microtubule architecture. The left panel shows representative images, the white arrows highlight the microtubule organising centre. Inset images highlight the centrosome-satellite region for a given image. The right panel shows the quantification of microtubule defects in cells that had been treated with either control or Ccdc13 siRNA (si1 or si2). (B) RPE-1 cells were transfected with non-targeting control siRNA, or two individual siRNAs (si1 or si2) that targeted Ccdc13, and then serum-starved for 48 h before fixation. Cells were then stained for PCNT and acetylated tubulin, and counterstained with DAPI (top panel). Bottom panel: the proportion of ciliated Ccdc13-depleted cells was quantified relative to control-siRNA-transfected cells. Inset images highlight the basal bodies for a given image. (C) Cell-cycle analyses of cells that had been treated with either control or Ccdc13-targeted siRNA, as indicated. (D) RPE-1 cells were transfected with a vector encoding YFP-tagged Ccdc13. After 24 h, cells were serum-starved for the indicated times before fixation, staining with antibodies recognising GFP and acetylated tubulin counterstaining with DAPI. White arrows highlight the site of the basal body, and inset images highlight the basal bodies for a given image. All experiments shown were performed at least three times, the error bars represent the standard error of the mean. Representative images are shown for each experiment.

Additionally, any role that Ccdc13 might have in interphase microtubule organisation appears to be independent of PCM1 satellite localisation, as PCM1 integrity was unaffected by Ccdc13 depletion (supplementary material Fig. S3C).

It has been shown previously that some centrosomal satellites, such as pericentrin, are required for efficient microtubule regrowth, where as others are not – i.e. PCM1 (Dammermann and Merdes, 2002; Dictenberg et al., 1998). To determine if Ccdc13 is required for this process, we assessed microtubule regrowth following rapid depolymerisation upon treatment with ice (Dammermann and Merdes, 2002). Cells that had been depleted of Ccdc13 exhibited increased microtubule regrowth, whereas cells that ectopically overexpressed Ccdc13, conversely, exhibited reduced microtubule regrowth following depolymerisation (supplementary material Fig. S3D). Additionally, we noted that YFP–Ccdc13 that had been disrupted following treatments with ice rapidly re-engaged with the centrosome during the early stages of microtubule re-polymerisation (supplementary material Fig. S3D). These data suggest that local concentrations of Ccdc13 around the microtubule organising centre might influence microtubule growth and, possibly, delay microtubule nucleation.

Many centriolar satellite proteins play crucial roles in cilium formation (Lopes et al., 2011; Stowe et al., 2012). Therefore, we depleted RPE-1 cells of Ccdc13 to examine a possible role for the protein in ciliogenesis. Ciliogenesis was induced in RPE-1 cells, by using serum withdrawal for 48 h, and confirmed by a pronounced increase in the proportion of ciliated cells, as assessed by positive staining for acetylated tubulin (Fig. 4B). Depletion of Ccdc13, using two individual siRNAs, caused a

Journal of Cell Science (2014) 127, 2910–2919 doi:10.1242/jcs.147785

substantial decrease in the proportion of ciliated cells (Fig. 4B). To confirm that this represents a specific effect, flow cytometric analyses and immunofluorescence studies showed that decreased ciliogenesis in Ccdc13-depleted cells was not caused by altered cell-cycle dynamics (Fig. 4C) or loss of PCM1 from the basal body (data not shown), respectively. In keeping with a functional role for Ccdc13 in ciliogenesis, we also observed that YFP–Ccdc13 localised to the basal body centriole pair following serum withdrawal, although YFP–Ccdc13 did not appear to localise to the cilium itself (Fig. 4D).

PCM1 and Cep290 are thought to cooperate with BBS4 to promote ciliogenesis (Kim et al., 2008; Lopes et al., 2011; Stowe et al., 2012). Given the severe effects of Ccdc13 depletion on ciliogenesis and the fact that it interacts with both PCM1 and Cep290 (Fig. 3A,C,D; supplementary material Fig. S2C), we proceeded to assess the effect of Ccdc13 depletion on the localisation of BBS4 using a previously established RPE-1-derived cell line that stably expressed LAP-tagged BBS4 (Nachury, 2008). siRNA-mediated knockdown of PCM1 was used as a positive control, and as expected, PCM1 depletion resulted in an almost complete loss of BBS4 localisation to both centriolar satellites and the primary cilium (Fig. 5A). Ccdc13 depletion also resulted in a decrease of BBS4 localisation to both centriolar satellites and the primary cilium (Fig. 5A), although this was less severe than that in PCM1-depleted cells (Fig. 5B). Because Ccdc13 depletion did not affect PCM1 localisation (supplementary material Fig. S3C), it might facilitate the ability of PCM1 to recruit BBS4 to centriolar satellites and, thus, aid cilia formation. However, because we do not have any evidence to suggest that Ccdc13 binds directly to BBS4 – it was not identified in our proteomic analyses of purified Ccdc13 complexes or detectable in coimmunoprecipitation studies – we suggest that this effect might be indirect. Collectively, these data indicate that although it does not appear to be essential for this process, Ccdc13 acts at the basal body to promote efficient cilia formation.

DISCUSSION

Here, we report the first characterisation of the human protein Ccdc13, which we identified in a human genome-wide siRNA screen for novel regulators of genome stability. Indeed, depletion of Ccdc13 leads to increased spontaneous levels of post-mitotic DNA damage. However, Ccdc13-depleted cells appear to have intact DDR mechanisms following exogenous insults. We, therefore, suggest that subtle microtubule defects in Ccdc13 cells enhance mitotic chromosome segregation errors, leading to an increased number of DNA breaks and activation of the DDR through previously described mechanisms (Janssen et al., 2011). Indeed, our proteomic analyses of purified Ccdc13 complexes suggest that it interacts with a number of centrosome and spindle proteins that are known to function in the maintenance of both interphase and mitotic microtubule organisation. These include PCM1 (Dammermann and Merdes, 2002), Cep90 (Kim et al., 2012; Kim and Rhee, 2011), CEP350 (Yan et al., 2006) and Cep290 (Kim et al., 2008; Lopes et al., 2011; Stowe et al., 2012). Given the non-toxic effects of Ccdc13 depletion, we predict that the majority of these lesions are repaired by NHEJ in the subsequent G1 phase of the cell cycle (Giunta et al., 2010), which is consistent with a lack of overt DDR defects in Ccdc13-depleted cells.

We also show here that Ccdc13 localised with PCM1 at pericentriolar satellites and that Ccdc13 was found at the centrosome and the basal body of primary cilia, revealing Ccdc13 as a newly identified centrosomal satellite protein. Centriolar satellites have been extensively studied in flies and mammals (Bärenz et al., 2011); they are electron-dense granules that are composed of numerous proteins that are involved in microtubule organisation and nucleation. These granules become more tightly localised to the centrosome throughout interphase before redistributing to the cytoplasm during metaphase. Like PCM1, Ccdc13 localised more tightly to the centrosome in late G2. By contrast, Ccdc13 remained centrosome-bound during

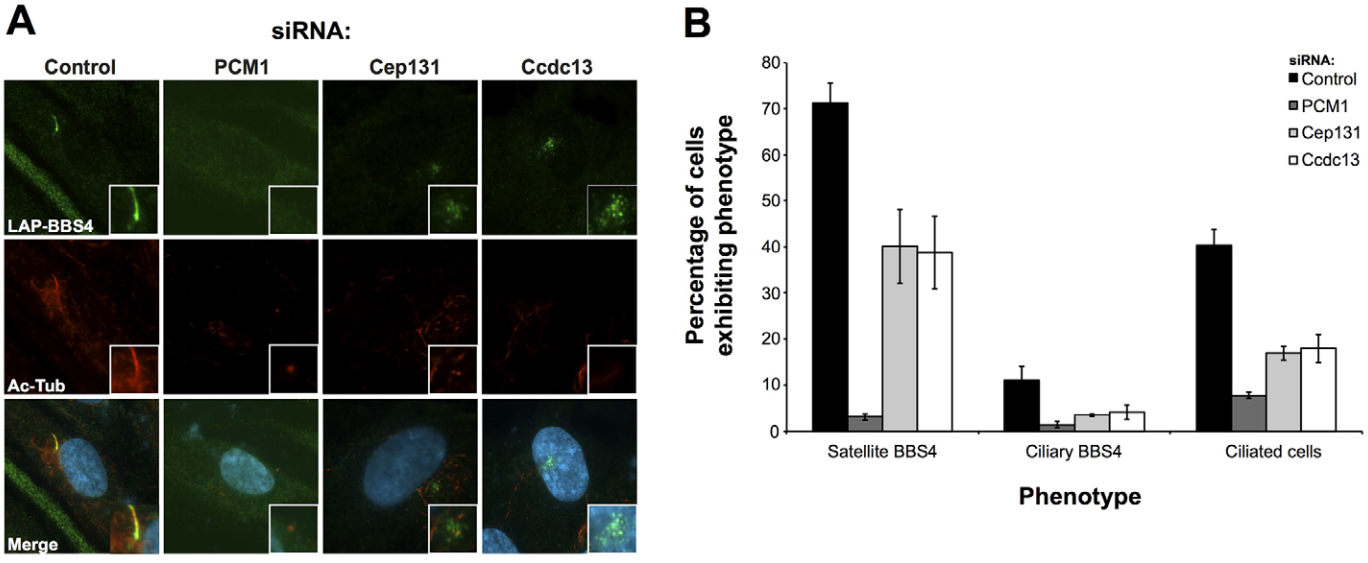

Fig. 5. Ccdc13 promotes BBS4 centriolar satellite localisation and ciliary recruitment. (A) RPE-1 cells that stably expressed LAP-tagged BBS4 were transfected with non-targeting control siRNA, or siRNA targeting PCM1, Cep131 or Ccdc13. After 48 h, the cells were fixed and stained for GFP and acetylated tubulin (Ac-Tub), and counterstained with DAPI (blue). Inset images highlight the basal bodies for a given image. (B) The proportion of cells with centriolar satellite BBS4 and ciliary BBS4 relative to cells that had been transfected with control siRNA, as determined from three independent experiments, error bars represent the standard error of the means.

Journal of Cell Science (2014) 127, 2910–2919 doi:10.1242/jcs.147785

metaphase and anaphase (Fig. 2B). Recent work has demonstrated that although a subset of satellite proteins – such as Cep131, PCM1 and BBS4 – are lost from the centrosome during mitosis (Balczon et al., 1994; Kim et al., 2004; Staples et al., 2012), others – including OFD1 and Cep290 – remain centrosomal during metaphase (Kim et al., 2008; Lopes et al., 2011; Stowe et al., 2012). The fact that Ccdc13 localisation to inter-phasic satellites but not the centrosome core was dependent on PCM1, suggests that specific and distinct protein complexes retain different Ccdc13 pools and/or sub-complexes within isolated centrosome compartments. Interestingly, we identified several uncharacterised coiled-coil domain-containing proteins in proteomic analyses of purified Ccdc13 complexes, suggesting that some of these might also be centrosomal satellites that facilitate the localisation of Ccdc13. Certainly, further characterisation of these coiled-coil domain-containing, in terms of centrosome biology and ciliogenesis, is worthy of future study.

It is well known that centriolar satellites participate in ciliogenesis (Lopes et al., 2011). We found that Ccdc13 localised to the basal body following serum withdrawal and remained associated with the basal body throughout ciliogenesis. Furthermore, Ccdc13 was required for cilia formation, although the observed defect was markedly less severe than that induced by PCM1 depletion (Fig. 5B). PCM1 is an absolute requirement for Cep290 and BBS4 localisation to centriolar satellites (Kim et al., 2008; Kim et al., 2004; Lopes et al., 2011). In turn, BBS4 is part of a protein complex termed the BBSome that promotes ciliogenesis by facilitating the Rabin8-dependent activation and ciliary localisation of the Rab8 GTPase (Kim et al., 2008). We observed decreased localisation of BBS4 to centriolar satellites in serum-starved RPE-1 cells that had been depleted of Ccdc13, without a concomitant effect on PCM1 or Cep290 localisation. This suggests that there is a specific role for Ccdc13 in the recruitment of BBS4 to centriolar satellites during ciliogenesis. However, from coimmunoprecipitation and proteomic studies, we do not have any compelling evidence that Ccdc13 and BBS4 interact (data not shown). Therefore, we suggest that Ccdc13 depletion alters the composition of centriolar satellites and, thus, decreases the ability of PCM1 to recruit BBS4. We are currently studying further the role of Ccdc13 in ciliogenesis by using a zebrafish mutant model, which will hopefully also yield potential insight into the functions of Ccdc13 in the development of organelles in which ciliogenesis is important (Malicki et al., 2011).

In conclusion, out data establishes Ccdc13 as a newly identified centrosomal satellite protein, which joins an increasing number of human centrosomal proteins – including Cep63, Cep131, Cep152, Cep164 and pericentrin – that are important for maintaining genome stability (Griffith et al., 2008; Kalay et al., 2011; Sivasubramaniam et al., 2008; Smith et al., 2009; Staples et al., 2012). Interestingly, several of these are either known, or putative, substrates for the key DDR regulating kinases ATM and ATR (Matsuoka et al., 2007; Smith et al., 2009), which might point to DDR-related regulation of these proteins. Collectively, these findings, together with recent genetic studies (Chaki et al., 2012; Choi et al., 2013; Kalay et al., 2011; Sivasubramaniam et al., 2008; Stiff et al., 2013; Valdés-Sánchez et al., 2013; Zhou et al., 2012), highlight emerging functional links between centrosomal satellites, the DNA damage response, genome stability and human ciliopathies (Chavali and Gergely, 2013). These findings open up new exciting avenues of research and suggest that mutations in other DDR-related proteins might be causal for a subset of human ciliopathies, and that, potentially, mutations in some centrosomal satellite proteins might be causal for a subset of cancer predisposition disorders.

MATERIALS AND METHODS

Antibodies

The following antibodies against the indicated proteins were purchased from Abcam: Cep131 (ab84864 for immunofluorescence, ab99379 for western blotting); phosphorylated RPA at residue Thr21 (ab61065), phosphorylated DNA-PKcs at residue Thr2609 (ab18356); a rabbit antibody against 53BP1 (ab36823); pericentrin (ab4448); Cep290 (ab85728); phosphorylated histone 3 at residue Ser10 (ab14955) and β-actin (ab8224). The following antibodies against the indicated proteins were purchased from Cell Signaling Technologies: phosphorylated γH2AX at residue Ser139 (no. 2577) and a rabbit antibody against PCM1 (Q-15, no. 5259). A mouse antibody against PCM1 (4152-B01) was purchased from Abnova. An antibody against phosphorylated γH2AX at residue Ser139 (JBW301, no. 05-636) was purchased from Millipore. A rabbit antibody against Rad51 (H-92) was purchased from Santa Cruz. For western blotting, primary antibodies were visualised using horseradish-peroxidase-conjugated secondary antibodies from DAKO. For immunofluorescence, antibodies against mouse or rabbit IgGs conjugated to Alexa Fluor 488 or Alexa Fluor 594 were used (Invitrogen).

Cell culture

HCT116, HeLa, U2OS and HEK293 cells were maintained as an adherent monolayer in Dulbecco's modified Eagle's medium that contained 10% FBS and 1% penicillin and streptomycin at 37℃ under a humidified atmosphere of 5% CO_2. HeLa Flp-in T-Rex and HEK293 Flp-In T-Rex cells (Invitrogen) were maintained in Dulbecco's modified Eagle's medium containing 10% FBS and 1% penicillin and streptomycin that had been supplemented with 4 µg/ml Blasticidin S (Melford) and 100 µg/ml Zeocin (Invitrogen). HeLa cells that stably expressed GFP-tagged histone 2B (H2B) were maintained in identical media that had been supplemented with 2 µg/ml Blasticidin S.

Stable cell line generation

Stable tetracycline-inducible HEK293 Flp-In cell lines that expressed cDNA encoding FLAG-tagged Ccdc13 (NM_144719.2) and HeLa Flp-In cell lines that expressed YFP- or FLAG-tagged Ccdc13 were generated by co-transfection of these cell lines with the pPGKFLPobpA-Flp recombinase and either empty pDEST-Flag/FRT/TO or pDEST-Flag/FRT/TO-Ccdc13, according to the Flp-In manufacturer's protocol. Recombinants were selected in medium that contained 4 µg/ml Blasticidin S and 150 µg/ml Hygromycin B (Invitrogen). All transient transfections were performed using Lipofectamine 2000 (Invitrogen), according to the manufacturer's instructions.

Transfections and drug treatments

HEK293, U2OS, RPE-1 and HeLa cells were transfected with between 30 and 50 nM siRNA using Lipofectamine 2000 (Invitrogen), RNAiMAX (Invitrogen) or Dharmafect 1 (Dharmacon), according to the manufacturer's instructions. Cells were collected, lysed or fixed for analysis after 48 h, unless otherwise indicated. The cells were treated with 1 µM nocodazole (Sigma) or 10 µM Taxol (Sigma) for 3 h, or 300 µM mimosine (Sigma), before fixation or release into drug-free medium for the indicated times.

Cell lysis and western blotting

For whole-cell extracts, the cells were solubilised on ice in lysis buffer (20 mM Tris-HCl pH 7.5, 150 mM NaCl, 1% Triton X-100, 1 mM dithiothreitol and 1 mM EDTA) supplemented with 50 U/µl benzonase (Novagen), and protease and phosphatase inhibitors (Sigma). Cleared lysates were produced by centrifugation of the resulting samples at 16,000 ***g*** for 15 min at 4℃. Gel electrophoresis was performed using the NuPAGE system (Invitrogen). Briefly, samples were resolved on 4–12% Bis-Tris gels in MOPS buffer, transferred to a PVDF membrane that was

then probed for the protein of interest using antibodies that had been diluted in PBS containing 5% fat-free milk and 0.1% Tween-20 (Sigma).

Immunoprecipitation

For purification of FLAG-tagged proteins, 1 mg of the whole-cell extract was incubated with 20 µl of M2 anti-FLAG beads (Sigma) for 16 h at 4℃. For immunoprecipitations using endogenous antibodies, 1–2 µg of antibody was incubated with the sample for 1–2 h before addition to 20 µl of washed Protein A/G beads (Santa Cruz) and incubation for 16 h at 4℃. Beads were then pelleted and washed three times in 20× the bed volume of the lysis buffer. The bound protein was eluted either by heating the beads at 95℃ for 5 min with 2×LDS buffer (Invitrogen) or by incubation with FLAG peptide (Sigma), according to manufacturer's instructions. Inputs represent ~1/40 of the extract that was used for the immunoprecipitation.

Immunofluorescence and live-cell imaging

Cells were grown on glass coverslips and treated as indicated, then fixed with either methanol or 3% buffered paraformaldehyde for 10 min at room temperature, and permeabilised in PBS containing 0.2% Triton X-100 for 5 min at room temperature. Cells were then incubated with primary antibody for 2 h at room temperature and detected with a secondary Alexa-Fluor-488- or Alexa-Fluor-594-conjugated goat anti-rabbit or anti-mouse IgG. Antibody dilutions and washes after incubations were performed in PBS. DNA was stained with DAPI (1 µg/ml), and coverslips were mounted in Shandon Immu-Mount medium (Thermo). Fluorescence microscopy was performed on a Nikon Eclipse T200 inverted microscope (Melville), equipped with a Hamamatsu Orca ER camera, a 200 W metal arc lamp (Prior Scientific, UK) and a ×100 objective lens. Images were captured and analysed by using Volocity 3.6.1 software (Improvision).

For live-cell imaging, H2B–GFP HeLa cells were grown on 24-well glass-bottomed plates (Scientific Laboratory Supplies) in selective medium. The cells were transfected with siRNA and then imaged on a Leica AF6000 LX inverted microscope that was fitted with an environmental chamber, set at 37℃ providing humidity and 5% CO_2. Leica LAS AF Lite software was used for image acquisition and analysis.

Cell-cycle analyses by using flow cytometry

Cells were trypsinised from the dishes and pelleted, then washed with PBS and fixed in 70% ice-cold ethanol. Cells were then washed with PBS and stained with a propidium iodide solution (50 µg/ml) containing RNase A (25 µg/ml) for 30 min before flow cytometry was performed using a Becton Dickinson FACScalibur instrument. Cells were gated for size and granularity to remove cell debris from the analyses, and 10,000 live cells were quantified for each treatment per experiment.

Acknowledgements

H2B-GFP HeLa cells were a kind gift from Peter Cook (Dunn School of Pathology, Oxford University, UK) and LAP-tagged BBS4 RPE-1 cells were a kind gift from Maxence Nachury (Stanford University, Stanford, CA). pEGFP-C1-p50-dynamitin was a kind gift from Andreas Merdes (University of Toulouse, France). The rabbit Cep215 antibody was a kind gift from Erich Nigg (University of Basel, Switzerland). We thank Helen Bryant and Mark Meuth for insightful discussions regarding this work.

Competing interests

The authors declare no competing interests.

Author contributions

C.J.S. and S.J.C. designed the experiments, prepared the figures and wrote the manuscript, with editing help from S.J.B. C.J.S. carried out the majority of the experiments with additional help from K.N.M., R.D.D.B., A.P., A.E.H. and G.B. A.J.X.L., C.S. and M.H. carried out the H2AX siRNA screen. S.M. and J.M.S. carried out proteomic analyses of purified FLAG-Ccdc13 complexes.

Funding

This work was supported by funding from Cancer Research UK (CR-UK) and Yorkshire Cancer Research (YCR). S.J.C. is the recipient of a CR-UK Senior Cancer Research Fellowship. C.J.S., K.N.M., A.J.X.L., C.S., M.H., S.J.B. and S.J.C. are funded by CR-UK. R.D.D.B., A.A.P. and G.B. are funded by YCR.

Supplementary material

Supplementary material available online at
http://jcs.biologists.org/lookup/suppl/doi:10.1242/jcs.147785/-/DC1

References

Balczon, R., Bao, L. and Zimmer, W. E. (1994). PCM-1, A 228-kD centrosome autoantigen with a distinct cell cycle distribution. *J. Cell Biol.* **124**, 783-793.

Bärenz, F., Mayilo, D. and Gruss, O. J. (2011). Centriolar satellites: busy orbits around the centrosome. *Eur. J. Cell Biol.* **90**, 983-989.

Bekker-Jensen, S., Lukas, C., Kitagawa, R., Melander, F., Kastan, M. B., Bartek, J. and Lukas, J. (2006). Spatial organization of the mammalian genome surveillance machinery in response to DNA strand breaks. *J. Cell Biol.* **173**, 195-206.

Bonner, W. M., Redon, C. E., Dickey, J. S., Nakamura, A. J., Sedelnikova, O. A., Solier, S. and Pommier, Y. (2008). GammaH2AX and cancer. *Nat. Rev. Cancer* **8**, 957-967.

Chaki, M., Airik, R., Ghosh, A. K., Giles, R. H., Chen, R., Slaats, G. G., Wang, H., Hurd, T. W., Zhou, W., Cluckey, A. et al. (2012). Exome capture reveals ZNF423 and CEP164 mutations, linking renal ciliopathies to DNA damage response signaling. *Cell* **150**, 533-548.

Chapman, J. R., Taylor, M. R. and Boulton, S. J. (2012). Playing the end game: DNA double-strand break repair pathway choice. *Mol. Cell* **47**, 497-510.

Chavali, P. L. and Gergely, F. (2013). Cilia born out of shock and stress. *EMBO J.* **32**, 3011-3013.

Choi, H. J., Lin, J. R., Vannier, J. B., Slaats, G. G., Kile, A. C., Paulsen, R. D., Manning, D. K., Beier, D. R., Giles, R. H., Boulton, S. J. et al. (2013). NEK8 links the ATR-regulated replication stress response and S phase CDK activity to renal ciliopathies. *Mol. Cell* **51**, 423-439.

Dammermann, A. and Merdes, A. (2002). Assembly of centrosomal proteins and microtubule organization depends on PCM-1. *J. Cell Biol.* **159**, 255-266.

Dictenberg, J. B., Zimmerman, W., Sparks, C. A., Young, A., Vidair, C., Zheng, Y., Carrington, W., Fay, F. S. and Doxsey, S. J. (1998). Pericentrin and gamma-tubulin form a protein complex and are organized into a novel lattice at the centrosome. *J. Cell Biol.* **141**, 163-174.

Giunta, S., Belotserkovskaya, R. and Jackson, S. P. (2010). DNA damage signaling in response to double-strand breaks during mitosis. *J. Cell Biol.* **190**, 197-207.

Griffith, E., Walker, S., Martin, C. A., Vagnarelli, P., Stiff, T., Vernay, B., Al Sanna, N., Saggar, A., Hamel, B., Earnshaw, W. C. et al. (2008). Mutations in pericentrin cause Seckel syndrome with defective ATR-dependent DNA damage signaling. *Nat. Genet.* **40**, 232-236.

Janssen, A., van der Burg, M., Szuhai, K., Kops, G. J. and Medema, R. H. (2011). Chromosome segregation errors as a cause of DNA damage and structural chromosome aberrations. *Science* **333**, 1895-1898.

Kalay, E., Yigit, G., Aslan, Y., Brown, K. E., Pohl, E., Bicknell, L. S., Kayserili, H., Li, Y., Tüysüz, B., Nürnberg, G. et al. (2011). CEP152 is a genome maintenance protein disrupted in Seckel syndrome. *Nat. Genet.* **43**, 23-26.

Kim, K. and Rhee, K. (2011). The pericentriolar satellite protein CEP90 is crucial for integrity of the mitotic spindle pole. *J. Cell Sci.* **124**, 338-347.

Kim, J. C., Badano, J. L., Sibold, S., Esmail, M. A., Hill, J., Hoskins, B. E., Leitch, C. C., Venner, K., Ansley, S. J., Ross, A. J. et al. (2004). The Bardet-Biedl protein BBS4 targets cargo to the pericentriolar region and is required for microtubule anchoring and cell cycle progression. *Nat. Genet.* **36**, 462-470.

Kim, J., Krishnaswami, S. R. and Gleeson, J. G. (2008). CEP290 interacts with the centriolar satellite component PCM-1 and is required for Rab8 localization to the primary cilium. *Hum. Mol. Genet.* **17**, 3796-3805.

Kim, K., Lee, K. and Rhee, K. (2012). CEP90 is required for the assembly and centrosomal accumulation of centriolar satellites, which is essential for primary cilia formation. *PLoS ONE* **7**, e48196.

Kodani, A., Tonthat, V., Wu, B. and Sütterlin, C. (2010). Par6 alpha interacts with the dynactin subunit p150 Glued and is a critical regulator of centrosomal protein recruitment. *Mol. Biol. Cell* **21**, 3376-3385.

Lee, S. and Rhee, K. (2010). CEP215 is involved in the dynein-dependent accumulation of pericentriolar matrix proteins for spindle pole formation. *Cell Cycle* **9**, 775-784.

Logan, C. V., Abdel-Hamed, Z. and Johnson, C. A. (2011). Molecular genetics and pathogenic mechanisms for the severe ciliopathies: insights into neurodevelopment and pathogenesis of neural tube defects. *Mol. Neurobiol.* **43**, 12-26.

Lopes, C. A., Prosser, S. L., Romio, L., Hirst, R. A., O'Callaghan, C., Woolf, A. S. and Fry, A. M. (2011). Centriolar satellites are assembly points for proteins implicated in human ciliopathies, including oral-facial-digital syndrome 1. *J. Cell Sci.* **124**, 600-612.

Ma, L. and Jarman, A. P. (2011). Dilatory is a Drosophila protein related to AZI1 (CEP131) that is located at the ciliary base and required for cilium formation. *J. Cell Sci.* **124**, 2622-2630.

Malicki, J., Avanesov, A., Li, J., Yuan, S. and Sun, Z. (2011). Analysis of cilia structure and function in zebrafish. *Methods Cell Biol.* **101**, 39-74.

Matsuoka, S., Ballif, B. A., Smogorzewska, A., McDonald, E. R., III, Hurov, K. E., Luo, J., Bakalarski, C. E., Zhao, Z., Solimini, N., Lerenthal, Y. et al. (2007). ATM and ATR substrate analysis reveals extensive protein networks responsive to DNA damage. *Science* **316**, 1160-1166.

Mogensen, M. M., Malik, A., Piel, M., Bouckson-Castaing, V. and Bornens, M. (2000). Microtubule minus-end anchorage at centrosomal and non-centrosomal sites: the role of ninein. *J. Cell Sci.* **113**, 3013-3023.

Nachury, M. V. (2008). Tandem affinity purification of the BBSome, a critical regulator of Rab8 in ciliogenesis. *Methods Enzymol.* **439**, 501-513.
Prosser, S. L., Straatman, K. R. and Fry, A. M. (2009). Molecular dissection of the centrosome overduplication pathway in S-phase-arrested cells. *Mol. Cell. Biol.* **29**, 1760-1773.
Sivasubramaniam, S., Sun, X., Pan, Y. R., Wang, S. and Lee, E. Y. (2008). Cep164 is a mediator protein required for the maintenance of genomic stability through modulation of MDC1, RPA, and CHK1. *Genes Dev.* **22**, 587-600.
Smith, E., Dejsuphong, D., Balestrini, A., Hampel, M., Lenz, C., Takeda, S., Vindigni, A. and Costanzo, V. (2009). An ATM- and ATR-dependent checkpoint inactivates spindle assembly by targeting CEP63. *Nat. Cell Biol.* **11**, 278-285.
Staples, C. J., Myers, K. N., Beveridge, R. D., Patil, A. A., Lee, A. J., Swanton, C., Howell, M., Boulton, S. J. and Collis, S. J. (2012). The centriolar satellite protein Cep131 is important for genome stability. *J. Cell Sci*. **125**, 4770-4779.
Stiff, T., Alagoz, M., Alcantara, D., Outwin, E., Brunner, H. G., Bongers, E. M., O'Driscoll, M. and Jeggo, P. A. (2013). Deficiency in origin licensing proteins impairs cilia formation: implications for the aetiology of Meier-Gorlin syndrome. *PLoS Genet.* **9**, e1003360.
Stowe, T. R., Wilkinson, C. J., Iqbal, A. and Stearns, T. (2012). The centriolar satellite proteins Cep72 and Cep290 interact and are required for recruitment of BBS proteins to the cilium. *Mol. Biol. Cell* **23**, 3322-3335.
Valdés-Sánchez, L., De la Cerda, B., Diaz-Corrales, F. J., Massalini, S., Chakarova, C. F., Wright, A. F. and Bhattacharya, S. S. (2013). ATR localizes to the photoreceptor connecting cilium and deficiency leads to severe photoreceptor degeneration in mice. *Hum. Mol. Genet.* **22**, 1507-1515.
Yan, X., Habedanck, R. and Nigg, E. A. (2006). A complex of two centrosomal proteins, CAP350 and FOP, cooperates with EB1 in microtubule anchoring. *Mol. Biol. Cell* **17**, 634-644.
Zhou, W., Otto, E. A., Cluckey, A., Airik, R., Hurd, T. W., Chaki, M., Diaz, K., Lach, F. P., Bennett, G. R., Gee, H. Y. et al. (2012). FAN1 mutations cause karyomegalic interstitial nephritis, linking chronic kidney failure to defective DNA damage repair. *Nat. Genet.* **44**, 910-915.